Journal of *Marine Science and Engineering*

MDPI

Article

Arrhenius Equation-Based Model to Predict Lithium-Ions Batteries' Performance

Liteng Zeng, Yuli Hu, Chengyi Lu *, Guang Pan and Mengjie Li

School of Marine Science and Technology, Northwestern Polytechnical University, Xi'an 710072, China
* Correspondence: luchengyi@nwpu.edu.cn

Abstract: The accuracy of Peukert's battery capacity equation may decrease under the conditions of variable current and variable temperatures. Some researchers have previously tried to overcome the lack of C-rate change. However, the dependence of battery capacity on temperature is still not included. In this paper, we mainly studied the capacity reduction effect of batteries under variable temperatures. The proposed method can calculate the battery's available capacity according to the specific discharge conditions. The experimental method proposed in this paper provides a reasonable test method to generate the required coefficients in order to establish a state of charge prediction model with high accuracy. After establishing the method, we can make a real-time prediction of the available energy of battery including the remaining energy of battery. From the result, we can see that the result is of great precision and the method is valuable.

Keywords: lithium-ion battery; Peukert's equation; temperature; available energy

Citation: Zeng, L.; Hu, Y.; Lu, C.; Pan, G.; Li, M. Arrhenius Equation-Based Model to Predict Lithium-Ions Batteries' Performance. *J. Mar. Sci. Eng.* **2022**, *10*, 1553. https://doi.org/10.3390/jmse10101553

Academic Editor: Mohamed Benbouzid

Received: 27 September 2022
Accepted: 19 October 2022
Published: 20 October 2022

1. Introduction

According to the power type, autonomous underwater vehicles (AUVs) can be divided into thermal power and electric power. The electric-powered underwater vehicle has excellent advantages over thermal-powered underwater vehicles in structure and performance, so it has developed rapidly in recent years [1]. Compared with the thermal-powered underwater vehicle, the electric-powered underwater vehicle has low noise, almost no track, and the navigation depth hardly affects its performance. It also has more advantages in structure, cost, and maintenance. Therefore, more and more countries adopt the electric power mode. The power system is the heart of the underwater vehicle, and the power battery is the most important part of the power system. Therefore, the research of power batteries is significant for the development and application of underwater vehicles. Lithium-ion batteries have a high energy density, high working voltage, low self-discharging rate, and convenient use and maintenance compared with other secondary batteries. In recent years, lithium-ion batteries have been widely used in the fields of electronic products, vehicles, aerospace and so on [2–4]. So far, most underwater vehicles have used lithium-ion batteries as their power system. In order to ensure the safety and reliability of the battery system, the basic state of the battery, SOC (state of charge) [5,6], the SOP (state of power) [7], and the SOH (state of health) [8,9], should be continuously monitored. The health status and available capacity of lithium-ion batteries will be significantly affected by temperature. Considering the special working environment of the AUV's power battery pack, which includes the confined space caused by deep water and high pressure, there is great difficulty in heat dissipation. That will lead to the battery working under high temperatures [10]. Therefore, it is urgent to carry out research about the impact of different temperatures on the performance of lithium-ion batteries.

In order to study the influence of discharge heat generation on the lithium-ion battery pack, it is necessary to establish the system temperature field in the discharging process.

Then, we need to analyze how the discharge performance is affected by temperature. Many researchers are committed to studying the thermal model to determine the temperature distribution of the battery. Bernardi et al. first established the general thermal model [11] of the battery system based on energy balance. They believe that the battery temperature results from the interaction between Joule heat, mixing heat, phase change heat, and electrochemical reaction heat. Assuming that the temperature distribution is uniform and changes with time, the heating rate can be calculated. Rao and Newman proposed a simplified thermal model to determine the heating rate of the battery system. In their research, the effects of mixing heat and phase change heat were ignored [11]. Using the thermal model proposed by Bernardi et al., Dong and Baek of Seoul National University, Korea, studied the heating mechanism of the battery [12]. The results show that under the condition of high-rate discharge, irreversible Joule heat is dominant. In contrast, under the condition of low-rate discharge, the reversible entropy heat generated by the electrochemical reaction is the primary heat generation. Forgez et al. of the Technical University of Compigne, France, established the lumped parameter thermal model of the cylindrical lithium-ion battery [13]. The model considered the resistive heat dissipation and reversible entropy heat generation of the battery, and calculated the battery's internal and external resistance by the steady-state method. Noboru Sato, of the Honda research center in Japan, considered three different kinds of heat: electrochemical reaction heat; polarization heat; and Joule heat [14]. They also studied the irreversible and reversible heat production difference with the depth of discharge DOD [15].

Compared with mature battery heat production and temperature field analysis, the research of how the electrical performance of battery cells is affected by temperature is relatively weak. In many applications it is essential to predict the SOC of the battery. All engineers build according to the SOC prediction method based on Peukert's equation. However, the equation has significant limitations. Unless the battery is discharged at a constant current and constant temperature, Peukert's equation cannot be used to accurately predict the residual capacity [16]. In practical cases, the battery will be discharged at different currents and experience various temperatures. In many occasions, Peukert's equation is used for power monitoring and supply systems [17]; however, the drastic change of discharging environment poses a challenge to this method. Because the average discharge current cannot accurately characterize the process of discharging, it is impossible to ensure that the battery's temperature remains constant during discharging. The error caused by the average current model may be quite large; therefore, it is necessary to introduce an equivalent power loss based on the real-time state to evaluate the battery state of charge.

Ryan O'Malley used an improved Peukert capacity model to study the available capacity of the battery [18]:

$$\Delta C_r = \gamma \left(\frac{I}{I_{ref}} \right)^m \left(\frac{T_{ref}}{T} \right)^n \quad (1)$$

where γ represents the measured electric discharged during a period of time. the ΔC_r represent the deduction of equivalent electricity during the time, T_{ref}. and I_{ref} represent the reference temperature value and reference current value. From the Equation (1), we can see with the increase of current and the decrease of temperature, the capacity deviation increases. The author believes that the effects of these factors are multiplicative rather than superposition, and the impact of temperature on chemical reaction rate is exponential [19]. Equation (1) shows that when the current of discharging increases, the reduction rate of effective capacitance increases. This is consistent with the commonly used Peukert equation. However, this model shows that with the decrease of battery temperature, the reduced effective capacity during discharge will also increase. Doerffel [20] illustrated this phenomenon in his article. This is because when the lithium-ion battery works at high temperatures, the diffusion of lithium-ion will accelerate, which will also accelerate the

internal side reactions of the lithium-ion battery, the capacity will increase slightly and the internal resistance will decrease slightly. In the process of charging and discharging at low temperatures, active lithium will deposit on the electrode surface. As the migration ability of lithium ion in the active electrode material and the conductivity of electrolyte decline, the capacity of lithium-ion battery will decrease rapidly and the internal resistance will increase sharply [21–24]. Therefore, the capacity and internal resistance of lithium batteries vary greatly at different temperatures.

If the battery size is large, Peukert's law may be distorted, because when the battery size is large the internal and external temperature difference will increase significantly, and the overall temperature of the battery will also be significantly affected by the discharging rate. In this case, only controlling the ambient temperature and investigating the influence of C-rate on the capacity of battery will lose precision.

2. Methods

Improved discharge capacity model: In order to improve Peukert's equation, a transformed method is proposed to define the available capacity of battery. In this paper, the available capacity of the battery is defined as the electricity discharged by the battery at a certain rate from the full state. When the output voltage of the battery reaches the cut-off voltage, it is regarded as the end of the discharging and the amount of electricity discharged in this process is defined as the available capacity of the battery. This assumption involves the absolute maximum residual capacity, which reaches zero when the discharge depth of the battery reaches 100% and can never be lower than this value. Considering the influence of various discharging conditions, the relational formula of how the discharging procedure affect the residual capacity can be listed as follows:

$$C_{\mathrm{r}}^{t+1} = C_{\mathrm{r}}^{t} - \Delta C_{\mathrm{r}} \tag{2}$$

where C_{r}^{t} is the effective capacity of the battery at time t, C_{r}^{t+1} indicating the effective capacity of the battery at time $t + 1$. As mentioned earlier, the loss of effective capacity of battery in each time will be affected by the discharging current (I) and battery temperature (T):

$$\Delta C_{\mathrm{r}} = k(I, T) \cdot \Delta \mathrm{C} \tag{3}$$

The coefficient k is to combine the reduced effective capacity with the measured electricity by multiplying the actual current by time. The value of k is related to the battery temperature and discharging current.

From the discharging data of experimental battery in this article, we can get the capacity-temperature relationship for the lithium-ion battery. At high temperature, the temperature variation has little effect on the battery capacity, but when the temperature reaches a lower range, the battery capacity will be more sensitive to the temperature variation. Therefore, conditions similar to Peukert's law should control this index. In this paper, an Arrhenius Equation about temperature T is introduced to characterize the equivalent capacity consumed by the battery at a certain time:

$$k(T) = b \cdot e^{\frac{-E_a}{R \cdot T}} + a \tag{4}$$

The parameters $(a,\ b, E_a)$ depend on the chemical and physical properties of the battery. These parameters determine the influence of temperature on the discharge capacity. However, the precise parameters of this model still need to be verified by experiments.

Battery available energy calculation model: When the battery capacity is known, the available energy of the battery needs to be calculated through the circuit model in combination with the open circuit voltage and discharge current of the battery. The typical battery model is shown in Figure 1. U_o and U_{ocv} are terminal voltage and open circuit voltage respectively:

$$U_o = U_{OCV} - (U_r + U_p) \tag{5}$$

where U_r and U_p are ohmic voltage and polarization voltage, respectively. It is assumed that the internal resistance is equal to the sum of ohmic resistance and polarization resistance. There is a threshold called cut-off voltage to ensure safe in the discharging process. U_o will drop to the cut-off voltage before U_{ocv}. The actual capacity of the battery is typically smaller than the maximum capacity, because of the voltage drop on the internal resistance. Since capacity, internal resistance, and discharge current have no effect on the open circuit voltage, the U_{ocv} of the battery is a function only about SOC [25,26]. U_{ocv} and SOC are assumed to obey the following formula:

$$\begin{array}{c} U_{ocv} = f(SOC) \\ SOC = f^{-1}(U_{ocv}) \end{array} \tag{6}$$

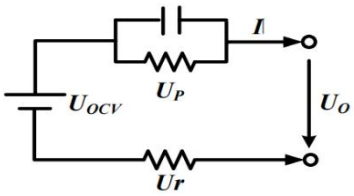

Figure 1. The model of circuit.

When the discharge process of the battery pack is cut off, the open circuit voltage of the battery cell is:

$$U_{OCV\text{-}Low} = U_{cut\text{-}off}(\text{dis}) + I \cdot R_s \tag{7}$$

where $U_{cut\text{-}off}$(dis) is the cut-off voltage of discharging and I is the discharging current of the battery pack. Among them $U_{ocv\text{-}Low}$ represent the lower limit of open circuit voltage in the discharging process. The lower SOC limit during discharging is:

$$SOC_L = f^{-1}(U_{ocv-Low}) \tag{8}$$

Therefore, during separate use, the SOC range of the battery cell during discharging is:

$$\Delta SOC = 100\% - SOC_L \tag{9}$$

Q represents the actual available capacity [27] of each battery under the discharging current I, C represent the theoretical capacity of battery cell regardless of the internal resistance:

$$\begin{array}{c} Q = \Delta SOC \times C \\ = C \cdot \left[100\% - f^{-1}\left(U_{cut\text{-}off(dis)} + I \cdot R_s\right)\right] \end{array} \tag{10}$$

Therefore, during battery discharging, the integral range is $SOC(U_{cut-off(dis)} + I \cdot R_s)$~100% Therefore, the available energy of the battery pack is:

$$E = \int_0^{t_0} U_{ocv}(SOC) \cdot Idt - \int_0^{t_0} R_s \cdot I^2 \cdot dt \tag{11}$$

When $t = 0$, $SOC = 100\%$, and when $t = t_0$, the discharging ends. If the variable of integration is converted from t to SOC, Equation (11) can be expressed as:

$$E = \int_{f^{-1}(U_{cut\text{-}off(dis)} + I \cdot R_j)}^{100\%} U_{ocv}(SOC) \cdot QdSOC - \int_0^{t_0} R_s \cdot I^2 \cdot dt \tag{12}$$

When the OCV curve, capacity and internal resistance of the battery are determined, the available output energy of the battery can be calculated quantitatively (Figure 2).

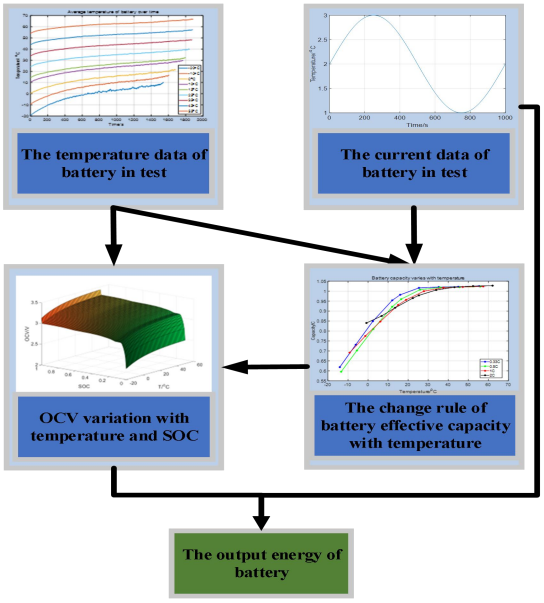

Figure 2. The flow chart of the proposed method to predict the output energy.

Experiment and data acquisition: In order to analysis the influence of temperature and discharge rate on the capacity and energy of the battery, we chose the LF105 battery as our experimental subject (Table 1). It is planned to conduct discharge experiments on the battery at nine different temperatures (−20 °C, −10 °C, 0 °C, 10 °C, 15 °C, 25 °C, 35 °C, 45 °C, and 55 °C) and four different rates (1/3C, 1/2C, 1C, and 2C). We used four batteries of the same type in the thermostat charged with four rates at the same time and each battery was performed nine cycles in the test. During the process, we used the thermostat shown in Figure 3 to ensure the temperature outside the battery, At the same time we measure the voltage and current of the batteries.

Table 1. The dimensions and basic parameters of LF105 battery.

Battery Type	Nominal Voltage	Nominal Capacity	Internal Resistance	Height	Width	Thickness	Electrode	Electrolyte
LF105	3.2 V	105 Ah	0.5 mΩ	200.5 mm	130.3 mm	36.7 mm	$LiFePO_4/C$	$LiPF_6$

We used thermocouples to record the temperatures of the positive, negative, and shell of the battery, respectively, every second. The places of the thermocouple mounting are shown in the Figure 3.

Firstly, according to the experimental data, four groups of curves can be obtained, such as the variation of capacity and energy of battery with ambient temperature and charging rate, which is shown in Figure 4. It can be seen from Figure 5a that when the ambient temperature is higher than 25 °C, the impact of the battery discharging rate on the battery capacity is very small and can be almost ignored. When the ambient temperature is lower than 25 °C, the battery capacity is greatly affected by temperature variation and the capacity shows a trend of first decreasing and then increasing with the increase of the discharging rate. We conclude that the average temperature of the battery has a significant impact on its capacity, because when the charging rate is large, the internal and external temperature difference will increase significantly. In the high-temperature stage, the capacity is less sensitive to the temperature variation between ambient temperature and battery temperature, while in the low-temperature stage, the capacity will be significantly affected by the temperature error. Because the effective capacity will be affected by the average temperature of battery, we define compensation coefficient k as shown in Equation (3). As shown in Equation (3), the author suggested a

hypothesis that the loss of effective capacity of battery in each time will be affected by the discharging current (I) and battery temperature (T). But through the experiment obtained, we can conclude that the current has little effect on the loss of effective capacity, even the little relation between them. This can also be explained as the current difference caused the temperature difference, and the temperature further affects the effective capacity.

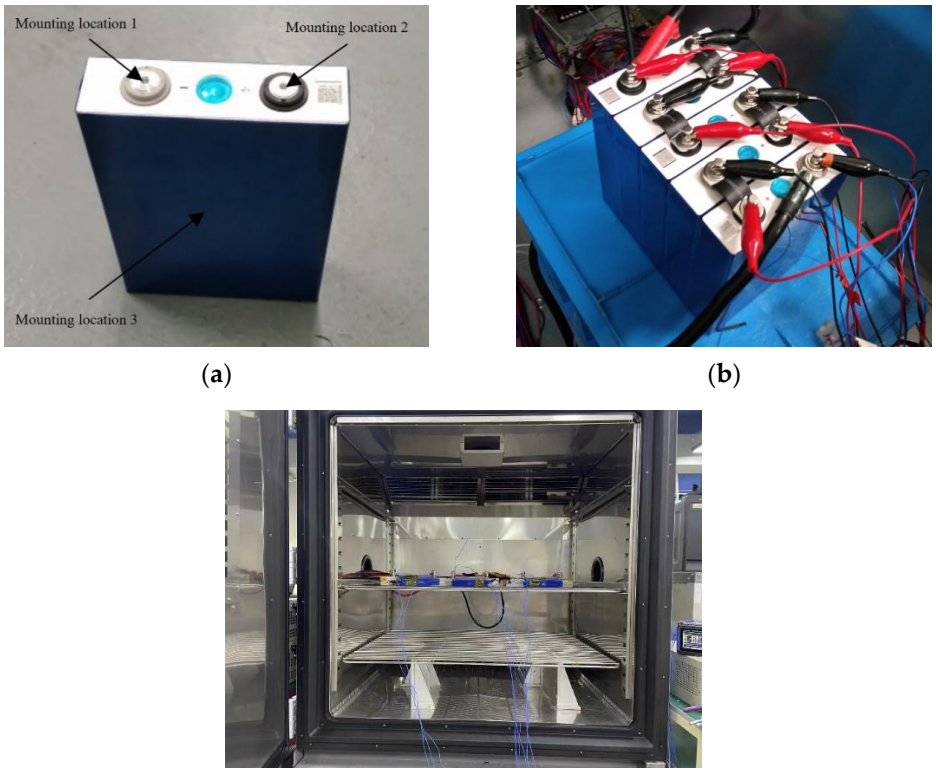

Figure 3. (**a**) The experimental subject LF105 battery. (**b**) The batteries in experiment. (**c**) The thermostat used in the experiment.

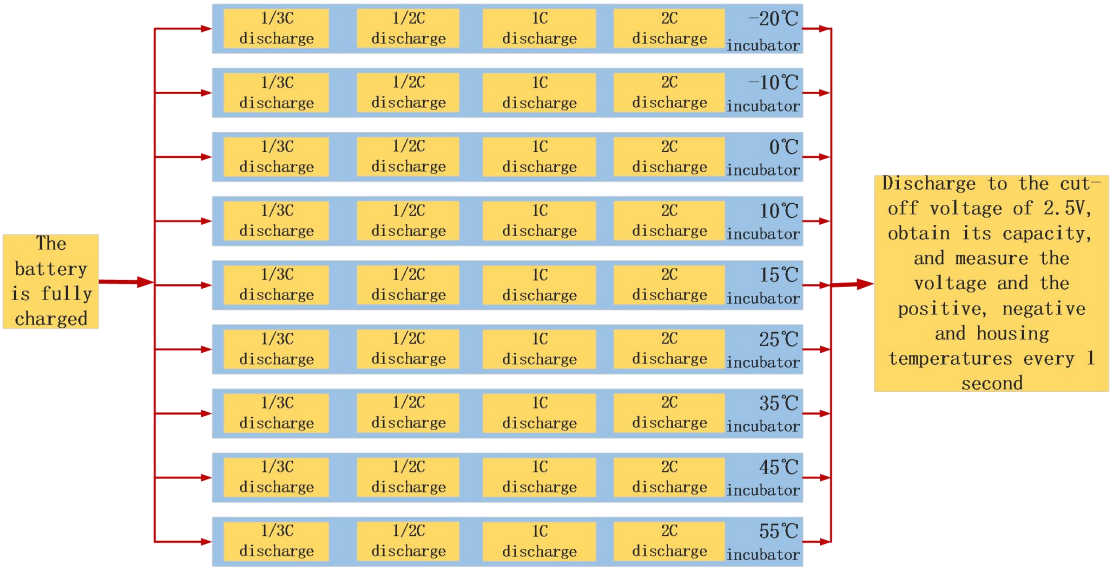

Figure 4. Schematic diagram of discharge experiment flow.

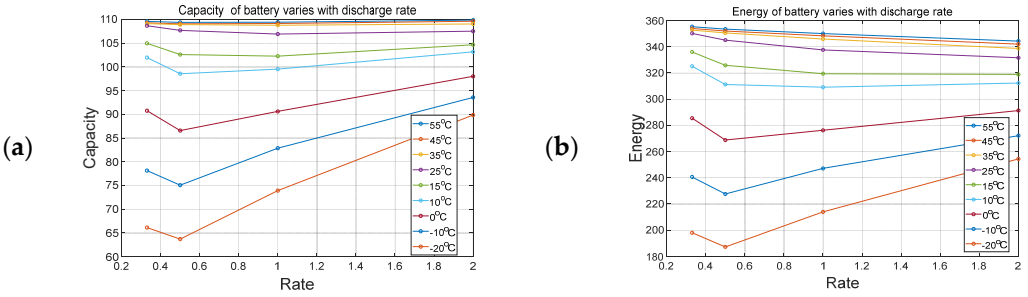

Figure 5. Variation of capacity and energy of battery with ambient temperature and charging rate.

Generally speaking, under the discharging rate of an electric vehicle, the capacity change is closely related to the self-generated heat [28]. There will still be a temperature differential between the center temperature and the surface temperature, even when a very high convective cooling rate is used to maintain the temperature of the battery [12]. Therefore, the ambient temperature cannot characterize the temperature of the battery precisely. Based of the above limitations, in order to keep the measured temperature close to the internal temperature of the battery as much as possible, this paper takes the average temperature on the positive pole, negative pole, and shell of the battery, at each time as the approximate temperature of the whole battery. We used the battery capacity at 25 °C and 1C discharging as the benchmark to obtain the capacity efficiency of the battery. The curve of capacity efficiency-battery temperature is shown in Figure 6.

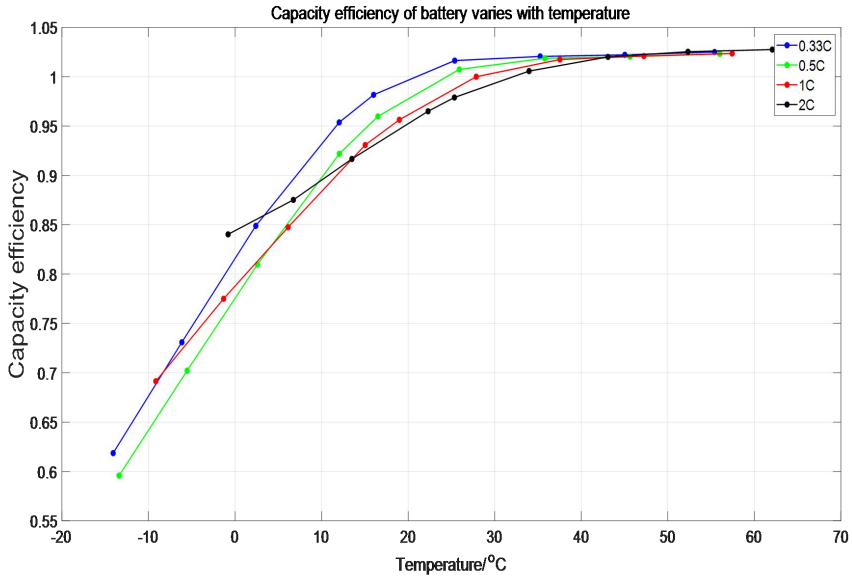

Figure 6. The capacity efficiency of the battery varies with the average temperature of the battery shell.

Data processing and calculation: in order to characterize the influence of temperature on battery capacity, the Arrhenius Equation (4) is used to fit the curve. Then, in order to obtain the corresponding parameters, the least square method is used to deal with the multiple linear regression problem.

It is assumed that there is the following linear relationship between variable y and variable $x_1, x_2, \cdots, x_m$:

$$Y = \beta_0 + \beta_1 x_1 + \cdots \beta_{mm} x_m + \varepsilon \tag{13}$$

In Equation (13), the parameters $\varepsilon \sim N(0, \sigma^2)$, β_0, $\beta_1, \cdots \beta_m, \sigma^2$ are unknown, and $m > 1$. Equation (13) is called multiple linear regression $x_1, x_2, \cdots, x_m$ are called regression variable and $\beta_0, \cdots, \beta_m$ are regression coefficient are regression coefficient. Setting

$(x_{i1}, x_{i2}, \cdots, x_{in}, Y_i)^T (i = 1, 2, \cdots, \mathrm{n})$ as n observations of $(x_1, x_2, \cdots, x_m, Y)^T$, then they meet the relationship:

$$Y_i = \beta_0 + \beta_1 x_{i1} + \cdots \beta_m x_{im} + \varepsilon_i \qquad i = 1, 2, \cdots, n \tag{14}$$

Assuming ε_i are independent with each other and satisfied $\varepsilon_i \sim N(0, \sigma^2), (i = 1, 2, \cdots, n)$.

Since the assumptions that ε_i are independent of each other, it can be seen from Equation (13) that Y_i are also independent of each other. Therefore, the mathematical expectation of Equation (13) can be expressed as follows:

$$EY = \beta_0 + \beta x_1 + \cdots \beta_m x_m \tag{15}$$

We call the equation:

$$\hat{Y} = \beta_0 + \beta_1 x_1 + \cdots \beta_m x_m \tag{16}$$

as a linear regression equation of Y about.$(x_1, x_2, \cdots, x_m)^T$.

In order to facilitate analysis about Equation (16), vector and matrix notation are introduced, then Equation (13) can be expressed in matrix form, we make $Y = (Y_1, Y_2, \cdots, Y_n)^{\mathrm{T}}$, $\beta = (\beta_1, \beta_2, \cdots, \beta_m)^T, \varepsilon = (\varepsilon_1, \varepsilon_2, \cdots, \varepsilon_n)^T$:

$$X = \begin{bmatrix} 1 & x_{11} & x_{12} & \cdots x_{1m} \\ 1 & x_{21} & x_{22} & \cdots x_{2m} \\ 1 & \vdots & \vdots & \vdots \\ 1 & x_{n1} & x_{n2} & \cdots x_{nm} \end{bmatrix} \tag{17}$$

Then Equation (13) can be expressed as:

$$Y = X\beta + \varepsilon \tag{18}$$

For Equation (18), the least square method is usually used to obtain $\hat{\beta}$,the estimator of β which meets the following conditions:

$$\sum_{i=1}^{n} \left(Y_i - \sum_{j=0}^{m} x_{ij} \hat{\beta}_j \right)^2 = min \sum_{i=1}^{n} \left(Y_i - \sum_{j=0}^{m} x_{ij} \beta_j \right)^2 \tag{19}$$

In general, the solution of (19) can be obtained by differential method as follows:

$$\sum_{i=1}^{n} \left(Y_i - \sum_{j=0}^{m} x_{ij} \hat{\beta}_j \right) x_{ik} = 0, k = 0, 1, \cdots, m \tag{20}$$

Expressed as a matrix, the system of Equation (20) can be written as:

$$X^T Y = \left(X^T X \right) \hat{\beta} \tag{21}$$

Since the rank of X is assumed to be m+1, $X^T X$ is positive definite, so there is an inverse matrix $\left(X^T X \right)^{-1}$, we can conclude from the above formula [29]:

$$\hat{\beta} = \left(X^T X \right)^{-1} X^T Y \tag{22}$$

By substituting the solution of $\hat{\beta}$ into the linear regression equation, we can get:

$$\hat{Y} = \hat{\beta}_0 + \hat{\beta}_1 x_1 + \cdots \hat{\beta}_m x_m \tag{23}$$

The above formula is the linear regression equation, through which Y can be predicted.

3. Model Fitting and Analysis

In order to use multiple linear regression for analysis, it is necessary to linearize the model expression (4). We take logarithms on both sides of the Equation (4) at the same time to obtain:

$$ln(1.032 - \mu) = \beta_0 - \beta_1 \cdot \frac{1}{T} \tag{24}$$

Among them:

$$\begin{aligned} \beta_0 &= ln(b) \\ \beta_1 &= ln(E_a/R) \end{aligned} \tag{25}$$

Compare with formula (16) we can get:

$$\begin{aligned} Y &= [\ln(1-\mu_1) \cdots \ln(1-\mu_n)]^{\mathrm{T}} \\ \beta &= [\beta_0, \beta_1]^{\mathrm{T}} \end{aligned} \tag{26}$$

$$X = \begin{bmatrix} 1 & -\frac{1}{T_1} \\ \vdots & \vdots \\ 1 & -\frac{1}{T_1} \end{bmatrix} \tag{27}$$

After solving the matrix, you can get β = [−21.4855,5417]. Substituting the obtained β into the formula, we can get $a = 1.032$, $b = 4.666 \times 10^{-10}$, $\frac{-E_a}{R} = 5417$ in Formula (4).

$$\Delta C_r = k(T) \cdot \Delta C = \frac{1}{1.032 - 4.666 \times 10^{-10} \times e^{(5417/T)}} \cdot idt \tag{28}$$

In order to verify the accuracy of the model, the equivalent electric quantity of the discharge process in various cases can be obtained (Figure 7).

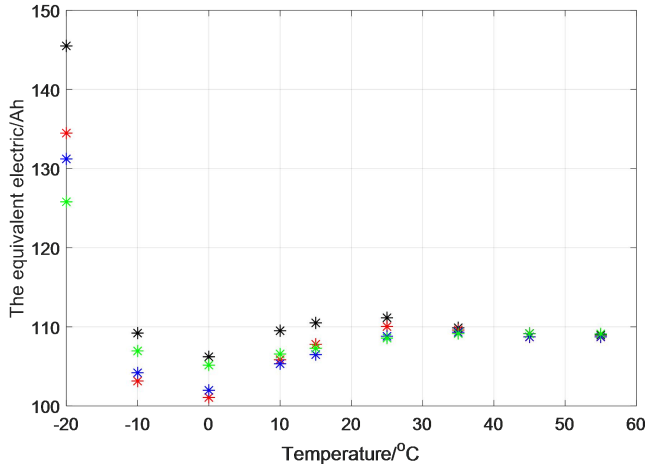

Figure 7. The equivalent electric discharged during the discharging process in various cases.

It can be seen from the table that if the quantity of electricity during discharging at different temperatures is calculated according to the equivalent algorithm, we can find that the equivalent capacity of the battery under every working condition almost maintains a constant value, except in the case at −20 °C. This shows that our equivalent capacity method is feasible in predicting the actual discharge capacity of the battery.

The comparison diagrams of the temperature trend of batteries at eight different ambient temperatures under the rates of 1/3C, 1/2C, 1C, and 2C, are also obtained, as shown in Figure 8. The capacity of the lithium-ion battery mainly depends on the temperature, and the temperature is affected by the discharge rate. The temperature of the battery may increase significantly, thereby increasing the available capacity under high current discharging rates. For the tests at high temperatures, the capacity of all tests remains

almost unchanged regardless of the discharging rate. This can be explained that during continuous high-speed discharging, the battery temperature exceeds 30 °C, which can enhance the performance of the lithium-ion battery. However, according to Arrhenius Equation (4), in the high temperature stage, the capacity of the battery is less affected by the temperature difference. In contrast, the battery temperature will not rise significantly under low-speed discharge, so the battery capacity will be greatly affected by the ambient temperature. Obviously, the rise of battery temperature is a function of environmental conditions, discharging rate, and battery design. Temperature is an important factor and should be considered when estimating the residual capacity of large-scale high-energy lithium-ion batteries.

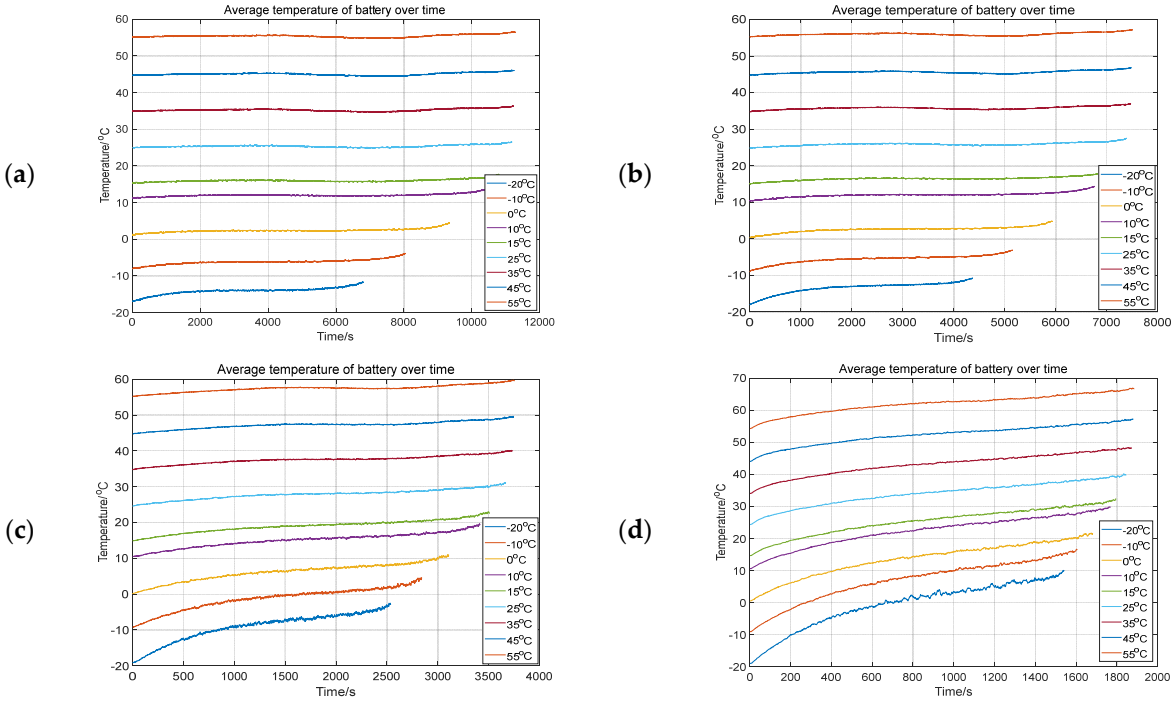

Figure 8. The temperature of the battery changes with time under the rate of (**a**) 1/3C, (**b**) 1/2C, (**c**)1C, (**d**) 2C.

As for the study of energy, the reduction of available energy caused by the increase of discharge current can be divided into two parts. The first part of energy reduction is caused by reaching the cut-off voltage in advance due to the increase of current, and the second part is caused by the rise of heat loss on the internal resistance of the battery due to the increase of current.

Therefore, when the open circuit voltage curve and internal resistance of the battery are determined, the available output energy of the battery can be calculated quantitatively.

It can be seen from the formula that at the same temperature, if the discharge ratio of the battery is high, the available energy will be reduced. The higher the discharging rate is, the lower of available energy is. Combined with the experimental data, it can be seen that the output energy efficiency of the battery changes with the average temperature, as shown in Figure 9.

The reaction activity of chemical substances inside the lithium-ion battery decreases at low temperature. The lower the temperature, the slower the chemical reaction, which is shown by the lower the battery voltage, The working voltage platform of the whole battery discharge will be reduced as a whole. In order to determine the U_{ocv} of the battery at other temperatures, the U_{ocv} of the battery at 55 °C is used as the reference voltage. It is known

that the output voltages of the battery U_1, the open circuit voltage U_{ocv} and the discharge current I_0 conform to the following relationship:

$$U_1 = U_{ocv}(SOC) - I_0 \cdot R_s \tag{29}$$

where I_0 is equal to the discharge current corresponding to the battery discharging at 1C rate. Accordingly, when the current is 2C:

$$U_2 = U_{\text{ocv}}\ (SOC) - 2 \cdot I_0 \cdot R_s \tag{30}$$

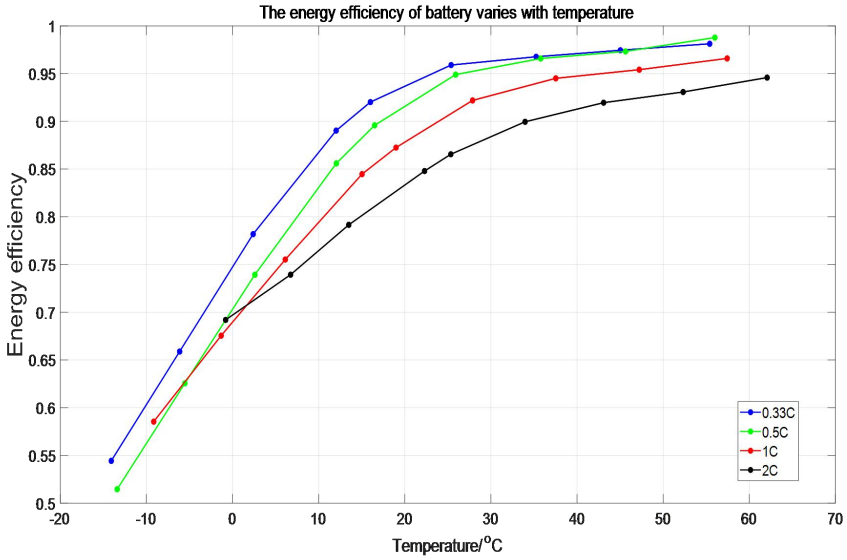

Figure 9. The energy efficiency of the battery varies with the average temperature of the battery shell.

The open circuit voltage curve U_{ocv} *(SOC)* of the battery at a specific ambient temperature can be solved by combining the above two formulas. It can be seen that when the ambient temperature is 55 °C, the *OCV-SOC* curve of the battery increases by 0.027 V compared with that when the ambient temperature is 25 °C, and the curve is similar to upward translation. The reason for this phenomenon may be that when the temperature is high, the chemical reaction inside the battery is more intense, resulting in higher open circuit voltage. In this paper, an approximate method is used to characterize the open circuit voltage of the battery at different temperatures. Firstly, the average operating voltage of the battery under 36 discharging conditions is obtained as listed in the Table 2 and Figure 10.

Table 2. The average output voltage of the battery under 36 discharging conditions.

Rates	55 °C	45 °C	35 °C	25 °C	15 °C	10 °C	0 °C	−10 °C	−20 °C
1/3C	3.2880	3.2590	3.2520	3.2429	3.2270	3.2175	3.1750	3.1069	3.0200
1/2C	3.2550	3.2480	3.2396	3.2274	3.2062	3.1920	3.1360	3.0620	2.9640
1C	3.2231	3.2141	3.2030	3.1861	3.1610	3.1470	3.0980	3.0470	2.9740
2C	3.1590	3.1452	3.1310	3.1121	3.0860	3.0737	3.0376	3.0012	2.9614

Then, the average open circuit voltage of the battery under various conditions is solved by fitting equations. Through MATLAB fitting, the expression of the average voltage of the battery with the ambient temperature can be given:

$$U_{mean} = -0.1377 \cdot e^{(-0.04225 \times T)} + 3.305 \tag{31}$$

In order to characterize the *OCV-SOC* curve of the battery under different SOC and different ambient temperatures, the *OCV-SOC* curve consist of the *OCV* at 55 °C and a

compensation difference are used. Based on the theoretical curve of the *OCV-SOC* curve under other operating conditions to estimate the output energy of the battery, which is shown in Figure 11.

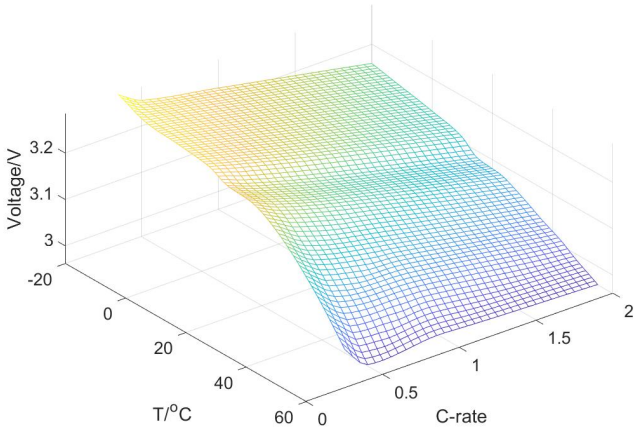

Figure 10. The output voltage of the battery varies with the ambient temperature and C-rate.

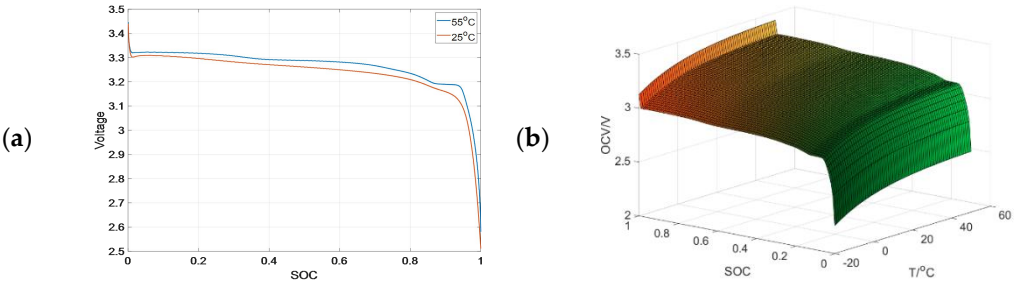

Figure 11. (**a**) Practical curve of battery OCV with battery SOC at different temperature. (**b**) Theoretical curve of battery OCV with battery SOC at different temperature.

We used the temperature data and current obtained during the discharge of the battery at different temperatures and rates. This can be used to calculate the output energy of the battery under specific conditions, in combination with the battery effective capacity estimation method, the OCV estimation method, and the output energy estimation method, mentioned in this paper. The comparison between the predicted value and the actual value of the battery output energy is as Figure 12. We can see that the predicted value of available energy is close to the real value.

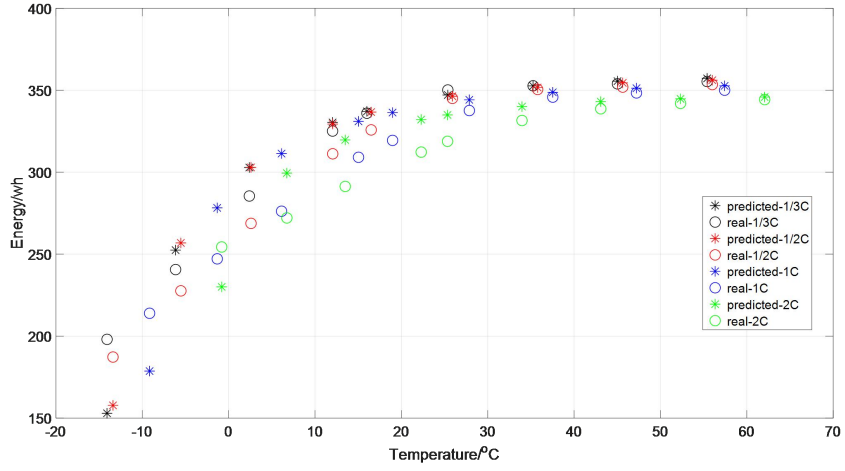

Figure 12. Prediction of output energy.

4. Conclusions

From the experiment data, we can conclude that: at low temperature, the viscosity of the lithium battery electrolyte increases. The activity of the active substance will be reduced when the conductivity is reduced. In addition, the diffusion rate of lithium ion in carbon anode will be relatively slow. It is very easy to have lithium precipitation, which will reduce the amount of recyclable lithium during charging and discharging, leading to the decline of battery capacity. Besides, the theory proposed in this paper is consistent with the practice, as shown in Figure 12. It can be seen that when the ambient temperature is higher than 30 °C, the output energy of the battery decreases with the increase of discharging rate, and the reduction degree increases with the discharging rate. At 10 °C and lower temperatures, the available energy of the battery does not decrease with the increase of C-rates because of the rise of battery capacity. The author believes that this phenomenon should be due to temperature differences. The average temperature of the positive and negative electrodes of the battery and the shell during the discharge process is taken as the overall average temperature of the battery. When the discharging of battery is large and the heat generation is intense, the temperature difference between the shell and the interior of the battery will be relatively large. Therefore, if the average temperature of the positive and negative electrodes and the shell is regarded as the overall temperature of the battery, a certain distortion will occur, resulting in a rise of the output energy at low temperature, as shown in the Figure 9.

In many applications, a reliable, accurate, and simple prediction of battery residual capacity is very important. In this article, we proposed a method to predict the residual capacity of batteries discharged with variable current based on a variant of Peukert's empirical equation, which links the available capacity to the constant discharge current. According to the test of lithium-ion power battery, the correlation between these technologies based on Peukert equation and the lithium-ion battery is also discussed. The basic conclusion of this paper is that Peukert's equation cannot be used to accurately predict the state of charge of the battery unless the battery is discharged at constant current and constant temperature. Only by applying the method proposed in this paper can we have a good prediction of the efficient capacity of battery. Combining the capacity model and the available energy calculation model, we can also make a good prediction of available energy based on the obtained data of temperature.

Author Contributions: Funding acquisition, Y.H. and G.P.; investigation, L.Z.; methodology, L.Z., C.L.; resources, M.L.; software, L.Z.; supervision, Y.H.; validation, M.L.; writing—original draft, L.Z.; writing—review and editing, C.L. All authors have read and agreed to the published version of the manuscript.

Funding: This research was supported by the National Natural Science Foundation of China (No. 21905231), and the Fundamental Research Funds for the Central Universities.

Institutional Review Board Statement: Not applicable.

Informed Consent Statement: Not applicable.

Data Availability Statement: Not applicable.

Conflicts of Interest: The authors declare no conflict of interest.

Nomenclature

I_{ref}	the reference current value.
T_{ref}	the reference temperature value.
γ	the measured electric discharged during a period of time.
m	the current coefficient.
n	the temperature coefficient.

I	the current value in practice.
T	the temperature value in practice.
C_{r}^{t+1}	the effective capacity of the battery at time t+1.
C_{r}^{t}	the effective capacity of the battery at time t.
ΔC_{r}	the deduction of equivalent electricity during the time
$k(I,T)$	coefficient to combine the reduced effective capacity with the measured electricity during discharging
ΔC	the deduction of measured electricity during the time
a	parameter related to the chemical and physical properties of the battery.
b	coefficient related to the chemical and physical properties of the battery.
E_a	a constant independent of temperature but related to the battery
R	Molar gas constant
U_o	terminal voltage (output voltage)
U_{OCV}	open circuit voltage
U_r	ohmic voltage
U_p	polarization voltage
R_s	the sum of Ohmic resistance and polarization resistance $(R_r + R_p)$
$U_{OCV\text{-}Low}$	the lower limit of open circuit voltage
$U_{cut\text{-}off}(\mathrm{dis})$	the cut-off voltage of discharging
SOC	the state of charge
SOC_L	lower SOC limit during discharging
ΔSOC	the range of variation of SOC during the discharging process.
Q	the electric discharged in the process of discharging
C	the theoretical capacity of battery cell regardless of the internal resistance
E	the available output energy of battery during discharging
t	time
$U_{ocv}(\mathrm{SOC})$	represent the open circuit voltage of battery under certain SOC
U_1	the output voltages of the battery under 1C discharging
U_2	the output voltages of the battery under 2C discharging
I_0	the current value corresponding to 1C discharging.
U_{mean}	the average open circuit voltage of the battery during discharging.

References

1. Wang, Y.-F.; Wu, J.-T. Performance improvement of thermal management system of lithium-ion battery module on purely electric AUVs. *Appl. Therm. Eng.* **2018**, *146*, 74–84. [CrossRef]
2. Wang, Y.; Zhang, C.; Chen, Z. An adaptive remaining energy prediction approach for lithium-ion batteries in electric vehicles. *J. Power Sources* **2016**, *305*, 80–88. [CrossRef]
3. Wang, Y.; Zhang, C.; Chen, Z. A method for joint estimation of state-of-charge and available energy of LiFePO 4 batteries. *Appl. Energy* **2014**, *135*, 81–87. [CrossRef]
4. He, H.W.; Zhang, Y.; Xiong, R.; Wang, C. A novel Gaussian model based battery state estimation approach: State-of-Energy. *Appl. Energy* **2015**, *151*, 41–48. [CrossRef]
5. Zhang, C.; Wang, L.Y.; Li, X.; Chen, W.; Yin, G.G.; Jiang, J. Robust and Adaptive Estimation of State of Charge for Lithium-Ion Batteries. *IEEE Trans. Ind. Electron.* **2015**, *62*, 4948–4957. [CrossRef]
6. Lin, C.; Mu, H.; Xiong, R.; Shen, W. A novel multi-model probability battery state of charge estimation approach for electric vehicles using H-infinity algorithm. *Appl. Energy* **2016**, *166*, 76–83. [CrossRef]
7. Sun, F.; Xiong, R.; He, H.; Li, W.; Aussems, J.E.E. Model-based dynamic multi-parameter method for peak power estimation of lithium–ion batteries. *Appl. Energy* **2012**, *96*, 378–386. [CrossRef]
8. Shen, W.X.; Chan, C.; Lo, E.; Chau, K. Adaptive neuro-fuzzy modeling of battery residual capacity for electric vehicles. *IEEE Trans. Ind. Electron.* **2002**, *49*, 677–684. [CrossRef]
9. Ouyang, M.; Feng, X.; Han, X.; Lu, L.; Li, Z.; He, X. A dynamic capacity degradation model and its applications considering varying load for a large format Li-ion battery. *Appl. Energy* **2016**, *165*, 48–59. [CrossRef]
10. Mao, Z.; Yan, S. Design and analysis of the thermal-stress coupled topology optimization of the battery rack in an AUV. *Ocean Eng.* **2018**, *148*, 401–411. [CrossRef]
11. Newman, J.; Bernardi, D.; Pawlikowski, E. A General Energy-Balance for Battery Systems. *J. Electrochem. Soc.* **1985**, *132*, 5.
12. Jeon, D.H.; Baek, S.M. Thermal modeling of cylindrical lithium ion battery during discharge cycle. *Energy Convers. Manag.* **2011**, *52*, 2973–2981. [CrossRef]
13. Forgez, C.; Do, D.V.; Friedrich, G.; Morcrette, M.; Delacourt, C. Thermal modeling of a cylindrical LiFePO4/graphite lithium-ion battery. *J. Power Sources* **2010**, *195*, 2961–2968. [CrossRef]

14. Sato, N. Thermal behavior analysis of lithium-ion batteries for electric and hybrid vehicles. *J. Power Sources* **2001**, *99*, 70–77. [CrossRef]
15. Lai, Y.; Du, S.; Ai, L.; Ai, L.; Cheng, Y.; Tang, Y.; Jia, M. Insight into heat generation of lithium ion batteries based on the electrochemical-thermal model at high discharge rates. *Int. J. Hydrogen Energy* **2015**, *40*, 13039–13049. [CrossRef]
16. Zhang, Q.; Cui, N.; Shang, Y.; Duan, B.; Zhang, C. An improved Peukert battery model of nonlinear capacity considering temperature effect. *IFAC-PapersOnLine* **2018**, *51*, 665–669. [CrossRef]
17. Rakhmatov, D.; Vrudhula, S.; Wallach, D.A. A model for battery lifetime analysis for organizing applications on a pocket computer. *IEEE Trans. Very Large Scale Integr. (VLSI) Syst.* **2003**, *11*, 1019–1030. [CrossRef]
18. O'Malley, R.; Liu, L.; Depcik, C. Comparative study of various cathodes for lithium ion batteries using an enhanced Peukert capacity model. *J. Power Sources* **2018**, *396*, 621–631. [CrossRef]
19. Ecker, M.; Gerschler, J.B.; Vogel, J.; Käbitz, S.; Hust, F.; Dechent, P.; Sauer, D.U. Development of a lifetime prediction model for lithium-ion batteries based on extended accelerated aging test data. *J. Power Sources* **2012**, *215*, 248–257. [CrossRef]
20. Doerffel, D.; Sharkh, S.A. A critical review of using the Peukert equation for determining the remaining capacity of lead-acid and lithium-ion batteries. *J. Power Sources* **2006**, *155*, 395–400. [CrossRef]
21. Liu, X.; Chen, Z.; Zhang, C.; Wu, J. A novel temperature-compensated model for power Li-ion batteries with dual-particle-filter state of charge estimation. *Appl. Energy* **2014**, *123*, 263–272. [CrossRef]
22. Fei, F.; Rengui, L.; Chunbo, Z. State of Charge Estimation of Li-Ion Battery at Low Temperature. *Trans. China Electrotech. Society* **2014**, *29*, 53–58.
23. Wang, H.W. Study of low temperature performance of Li-ion battery. *Battery Bimon.* **2009**, *39*, 208–210. Available online: https://www.semanticscholar.org/paper/Study-of-low-temperature-performance-of-Li-ion-Chang-bo/4079ca524a3959abc6e2bd061c4f2659d04ab570 (accessed on 20 September 2022).
24. Li, J.; Yuan, C.F.; Gao, Z.H.; Zhang, Z.A.; Lai, Y.Q.; Liu, J. Limiting factors for low-temperature performance of electrolytes in LiFePO4/Li and graphite/Li half cells. *Electrochim. Acta* **2012**, *59*, 69–74. [CrossRef]
25. Plett, G.L. Extended Kalman filtering for battery management systems of LiPB-based HEV battery packs: Part 2. Modeling and identification. *J. Power Sources* **2004**, *134*, 262–276. [CrossRef]
26. Lee, S.; Kim, J.; Lee, J.; Cho, B. State-of-charge and capacity estimation of lithium-ion battery using a new open-circuit voltage versus state-of-charge. *J. Power Sources* **2008**, *185*, 1367–1373. [CrossRef]
27. Diao, W.; Jiang, J.; Zhang, C.; Liang, H.; Pecht, M. Energy state of health estimation for battery packs based on the degradation and inconsistency. *Energy Procedia* **2017**, *142*, 3578–3583. [CrossRef]
28. Smith, K.; Wang, C.-Y. Power and thermal characterization of a lithium-ion battery pack for hybrid-electric vehicles. *J. Power Sources* **2006**, *160*, 662–673. [CrossRef]
29. Zhang, C.; Allafi, W.; Dinh, Q.; Ascencio, P.; Marco, J. Online estimation of battery equivalent circuit model parameters and state of charge using decoupled least squares technique. *Energy* **2018**, *142*, 678–688. [CrossRef]